Air Quality, Atmosphere & Health (2020) 13:593–605
https://doi.org/10.1007/s11869-020-00822-w

Two decades of ozone standard exceedances in Santiago de Chile

Rodrigo J. Seguel [1,2] · Laura Gallardo [1,2] · Zoë L. Fleming [1,2] · Sofía Landeros [1]

Received: 17 December 2019 / Accepted: 26 March 2020 / Published online: 8 April 2020

Abstract

A drastic decline of 2.4 ppbv decade^{-1} in the ozone mixing ratio has been measured in Santiago de Chile during the 2000s. Subsequently, in the 2010s, ozone trends stabilized in downtown and showed upward trends in eastern Santiago. The number of days with an 8-h average ozone mixing ratio above 61 ppbv, deemed harmful to health according to Chilean legislation, has declined significantly both in western and central Santiago. However, in eastern Santiago, one finds a 2010–2018 decade average of 43 days per year above recommended levels. Also, at a Receptor Site located ~ 70 km downwind from Santiago, this number rose to up to 3 months per year. A common denominator for the last two decades has been a steady increase in both gasoline and diesel-powered private cars. In the 2010s, the ozone weekend effect was frequently noted, providing evidence that the ozone formation regime in Santiago is VOC-limited. Nitrogen oxides and carbon monoxide (a proxy of anthropogenic VOCs) have increased steadily since 2014 in a relatively constant CO-to-NO_x ratio. Therefore, we propose that primary emissions of NO_X and VOCs from motor vehicle exhaust have remained as the main driver of the photochemical air pollution in Santiago as well as explaining the weekly variation. Santiago, like other megacities in the world, faces several challenges associated with increasing urbanization as well as the effects of climate change. An increasing population, growth in private car use, and urban sprawl have contributed to maintain high levels of ozone. New threats such as increasing temperatures observed in the central valleys of Chile, along with more frequent occurrences of heat waves, whose number has doubled in the last decade, will require a different approach to manage ozone pollution during the next decade. Santiago will not meet its own goals in the upcoming years without implementing robust, scientifically sound, and cost-effective strategies designed specifically to tackle photochemical pollution.

Keywords Ozone · Nitrogen dioxide · Photochemical pollution · Heat waves · Santiago

Introduction

Urban ozone (O_3) pollution has been an issue in several cities in the world because it impairs human lung function and induces inflammation of the respiratory tract above certain thresholds (e.g., Lippmann 1991; McConnell et al. 2002; Bell et al. 2004; Liu and Peng 2018; Entwistle et al. 2019). Dealing with O_3 pollution is complex because this pollutant is not emitted directly into the troposphere, but it is produced by volatile organic compounds (VOCs) in the presence of nitrogen oxides, i.e., $NO_x = NO + NO_2$ (Atkinson and Arey 1998, 2003). Besides, VOC precursors are derived from heterogonous sources, such as anthropogenic fossil fuels, solvents, aerosol products, and combustion processes, but also from biogenic emissions (Goldstein and Galbally 2007).

Additionally, during O_3 photochemical production, the oxidation of VOCs, initiated by hydroxyl radicals ($^{\bullet}OH$), contributes to the formation of secondary organic aerosols (SOA), a significant constituent of the fine particulate matter (PM) (Tsigaridis and Kanakidou 2018; Seguel et al. 2009; Paasonen et al. 2013), which is considered to be among the leading ten risk factors due to its adverse effects on human health (GBD 2016).

From a regional perspective, O_3 is also a matter of concern as its transport may impact on the ecosystem productivity and crop yields at downwind sites (Van Dingenen et al. 2009; Mills et al. 2018) and because secondary organic particles, together with O_3, affect climate forcing (Jimenez et al. 2009; Shrivastava et al. 2017; Scott et al. 2018).

✉ Rodrigo J. Seguel
rodrigoseguel@uchile.cl

[1] Center for Climate and Resilience Research (CR)2, Santiago, Chile

[2] Departamento de Geofísica, Facultad de Ciencias Físicas y Matemáticas, Universidad de Chile, Santiago, Chile

Santiago (33.5 S, 70.5 W, 540 m a.s.l.) has experienced high levels of O_3 since official air quality monitoring was established in late 1996 (Seguel et al. 2013; Seguel et al. 2018). The 8-h standard of 61 ppbv has been permanently exceeded (Rubio et al. 2004), and therefore, the Santiago Metropolitan Region was designated as a nonattainment area for O_3 in 1996. As a result of the implementation of several measures mainly oriented toward coarse particulate matter smaller than 10 μm in diameter (PM_{10}) (Barraza et al. 2017; Gallardo et al. 2018), the O_3 mixing ratios have decreased at several of Santiago's monitoring stations up until 2013. These measures include continued enhancement in fuel quality, introduction of catalytic converters, improvement in the public transportation system, enforcement of strict emission standards for vehicles, increasingly stringent industrial regulations, and an extension of the subway network (e.g., Gallardo et al. 2018; Mena-Carrasco et al. 2014). However, these promising results have been reached without measures specifically designed to curb photochemical pollution. For example, there is no routine monitoring of reactive VOCs, and the NO_2 standard has not been reduced since 2003. Currently, the 1-h standard for NO_2 (213 ppbv) in Chile is twice as high as the EU standard (106 ppbv) and the USA (100 ppbv) standard.

VOC campaigns in Santiago have been sparse and discontinuous over the last 20 years. Contributions have been made in 1996 and 2002 concerning urban photochemistry and the impact of anthropogenic VOCs on high O_3 levels (Rappenglück et al. 2000, 2005). Measurement campaigns carried out during 2005 and modeling determined that the photochemical O_3 formation in Santiago was VOC-limited and therefore the reduction of VOCs was found to be the most effective way of reducing O_3 mixing ratios in downtown Santiago (Elshorbany et al. 2009, 2010; Seguel et al. 2012). Later in 2009–2010, a photochemical study conducted in Santiago and its surrounding valleys showed that the O_3 can be transported large distances toward the northeast (Seguel et al. 2013; Toro et al. 2014, 2015). In this summer campaign, aromatics (m + p – xylene) were found as the species with the highest O_3 formation potential among anthropogenic VOCs, but also the diurnal mixing ratio of biogenic isoprene (2-methyl-1,3-butadiene, C_5H_8), ranging between 0.13 and 1.9 ppbv, showed a high O_3 forming potential due to its extremely high reactivity toward $^{\bullet}OH$ ($k = 1.01 \cdot 10^{-10}$ cm^3 $molecule^{-1}$ s^{-1}) (Atkinson and Arey 2003). In Santiago, the significant proportion of non-native deciduous trees versus native evergreen species results in higher emissions of highly reactive biogenic VOCs (BVOC) such as isoprene that impact on O_3 formation (Préndez et al. 2013).

Santiago, with more than 7 million inhabitants, is a city in continuous expansion. The urban area covers 838 km^2 (Gallardo et al. 2018) spread in a complex terrain that is almost entirely surrounded by the Andes Range to the East (~ 4.5 km a.s.l.) and by the Coastal Range to the West (~ 1.6 km a.s.l.) (Fig. 1a). Closely related with the growth of the city, the number of motor vehicles is also increasing and in 2018 reached 2,124,481 units (http://www.ine.cl/). Gasoline and diesel engines dominate respectively accounting for 78.6% and 21.1% of the vehicle fleet. Other fuels, such as liquefied petroleum gas (LPG) and natural gas (NG), are still low, accounting for only 0.2%. The number of electric vehicles is also extremely low (0.05%).

A major meteorological characteristic of Santiago is the quasi-permanent influence of the subtropical Pacific high, and the intrusion of occasional cold fronts, which bring precipitation in wintertime (Garreaud et al. 2009). The South Pacific High determines quasi-stagnant anti-cyclonic conditions that are further intensified, by the presence of subsynoptic features known as coastal lows (Gallardo et al. 2002; Garreaud et al. 2002). Summer surface circulation is mainly driven by topography and surface radiation and experiences only a minor modulation from the synoptic-scale circulation. Thus, Santiago shows a prevalent mountain-valley circulation that controls surface winds especially during the warm season. This thermally driven circulation defines upslope south-westerly winds in the afternoon and down-slope north-easterly winds during the night and at dawn (Saide et al. 2011).

Since 2010, Central Chile (30–38° S) has experienced a megadrought, affecting a geographical extension of about 900 km, with an annual rainfall deficit of 25–45% (Boisier et al. 2016, 2018). Moreover, temperature trends have shown a warming of + 0.25 °C per decade in the central valleys (Falvey and Garreaud 2009), and in the western foothills of the Andes range, this increase is even more extreme. Also, in recent years, heat waves have become more frequent, intense, and longer in Central Chile (Piticar 2018). Warmer summers and extreme temperatures have the potential to increase BVOC emissions from terrestrial ecosystems and therefore increase the formation of tropospheric O_3 (Lee et al. 2006). The latter has important implications not only for atmospheric chemistry but also for the compliance of the National Air Quality Standards (NAAQS) for O_3, and possibly $PM_{2.5}$, in Central Chile in general and Santiago in particular.

Consequently, in this study, we analyzed the trend of O_3 and NO_x in selected monitoring stations of the Santiago basin in order to understand 20 years of O_3 standard violations in the Santiago Metropolitan Region. Furthermore, we analyzed the role of NO_x in the temporal and spatial variability of O_3 in Santiago to provide information regarding the current O_3 formation regime and its more effective control over the next decade. Additionally, the implications of environmental factors such as temperature in the future compliance of the O_3 standard are discussed. Finally, the O_3 mixing ratios are used to assess the potential impact of O_3 on vegetation and crop productivity downwind of Santiago.

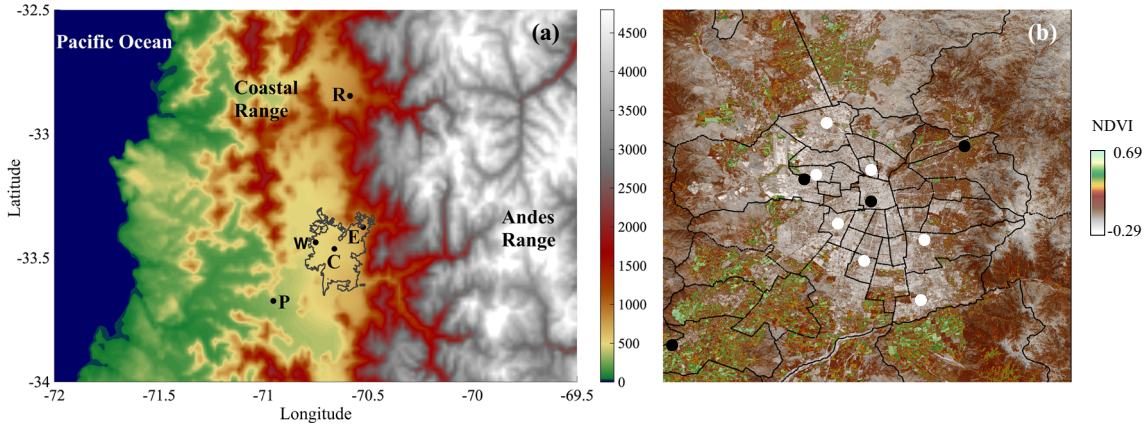

Fig. 1 **a** The left panel shows the topographic features of the study area. Black circles represent the location of the monitoring stations where P stands for Peri-urban Site (Talagante), W stand for Western Site (Pudahuel), C stands for Central Site (Parque O'Higgins), E stands for Eastern Site (Las Condes), and R stands for Receptor Site (Los Andes). The gray contour line represents the urban boundary of Santiago, and the left axis scale is the altitude in meters. **b** The right panel shows the average of the NDVI obtained from the satellite Sentinel at a 10 m of spatial resolution for the summers (December, January, February) of 2016–2017, 2017–2018, and 2018–2019. White circles represent other monitoring stations not included in this analysis. The black lines represent the city administrative divisions

Methodology

Surface observations (O_3, NO, NO_2, and CO)

The Ministry of the Environment routinely measures criteria pollutants O_3, NO, NO_2, CO, and surface meteorological variables at 11 sites of the Santiago basin (https://sinca.mma.gob.cl; Schultz et al. 2017). In this study, four monitoring stations were selected and assigned to represent the predominant wind direction during the hours of greatest photochemical activity. These locations were Talagante (33.674 S, 70.953 W, 341 m a.s.l.), Pudahuel (33.438 S, 70.750 W, 460 m a.s.l.), Parque O'Higgins (33.464 S, 70.661 W, 540 m a.s.l.), and Las Condes (33.377 S, 70.523 W, 795 m a.s.l.), hereafter referred to as Peri-urban Site, Western Site, Central Site, and Eastern Site, respectively. Additionally, the nearby (~ 70 km northeast) town of Los Andes (32.846 S, 70.587 W, 839 a.s.l.) was selected as a Receptor Site for photochemical pollution and hereafter referred to as Receptor Site (Fig. 1a).

Ozone is measured using continuous instruments based on a UV absorption technique (Thermo Scientific Inc. USA, www.thermoscientific.com, Model 49i). This analyzer has a minimum detection limit of 1.0 ppb, a response time of 10 s, and an absolute accuracy of 2%. NO_x is measured using a chemiluminescence analyzer (Thermo Scientific Inc. USA, Model 42i). NO_2 is converted to NO by a molybdenum converter heated to ~ 325 °C. This instrument has a minimum detection limit of 1.0 ppb, a response time of 120 s, and an absolute accuracy of 1%. CO is measured using an infrared absorption technique (Thermo Scientific Inc. USA, www.thermoscientific.com, Model 48i). The analyzer has a detection limit of 40 ppbv and an accuracy of 0.1%.

Descriptive statistical analyses of hourly measurements of O_3, NO, NO_2, and CO were performed using the open-source programming language R (R Development Core Team, Vienna, Austria) and its packages OpenAir (Carslaw 2013) and RStudio (RStudio Boston, MA, available from www.rstudio.org/). Most of the data used in this research has been validated by the Ministry of the Environment. Preliminary data were also included for recent years after quality checks that include the elimination of anomalous data and verification of detection limits. The TheilSen function of OpenAir was used to determine the deseasonalized trends for the time series. The function also provides the 95% confidence interval in the trend and the significance level (e.g., $p < 0.001$).

Assessment of the O_3 primary standard

The Chilean National Ambient Air Quality Standard (NAAQS) for ground-level O_3 is 61 ppbv based upon an 8-h average (http://bcn.cl/1xewl). Currently, attainment of the O_3 standard demands that the 3-year average of the 99th percentile of the maximum daily 8-h average (MDA8) O_3 mixing ratio does not exceed 61 ppbv.

Assessment of W126

Chile does not have an air quality standard aimed at protecting vegetation from ozone. Here, an explicit secondary index will be used to complement Chile's O_3 NAAQS, i.e., the W126 index proposed by Lefohn and Runeckles (1987). The W126 value is expressed as a sum of weighted hourly mixing ratios, cumulated over the 12-h daylight period from 8:00 to 19:00 local standard time (Eq. 1).

$$Daily \quad Index = \sum_{i=8:00}^{19:00} O_3 \times \left(\frac{1}{1 + (4403 \times e^{-126 \times O3i})} \right) \quad (1)$$

where O_{3i} is the hourly O_3 mixing ratio.

Then the monthly index is computed by summing all the daily index values in the month. Finally, the 3-year average is computed by averaging the maximum 3-month sum from each year in a 3-year period (US Federal register 2015).

Heat waves

The threshold temperature to distinguish between extreme and normal days uses the 90th percentile of the mean maximum temperature for each month calculated between 1961 and 1990 following the National Weather Service (DMC) guidelines (DMC 2018). Then, to identify heat waves, we applied the following definition: 3 or more consecutive days in which the maximum temperature exceeds the temperature threshold of Santiago. The thresholds of Santiago for December, January, and February are 31.9, 32.5, and 32.0 °C, respectively.

Results and discussion

Trends in O_3, NO, NO_2, and CO

Over the period 1 January 1998 to 31 March 2019 (~ 21 years), the central monitoring station shows a substantial decline in O_3 mixing ratio (Fig. 2). The aforementioned reduction exhibited a statistically significant negative trend of (−) 0.24 [0.30, 0.19] ppbv year^{-1} ($p < 0.001$) until 2013. However, after 2013, no significant trend for O_3 mixing ratio was observed. In contrast, since 2014, NO and NO_2 precursors showed a statistically significant positive trend of (+) 2.0 [1.2, 3.0] and (+) 2.4 [1.8, 3.3] ppbv year^{-1} with $p < 0.001$, respectively.

The latest official inventory of Santiago (USACH 2014), as well as demonstrating the increasing number of motor vehicles, is insightful for understanding the positive trend in NO_x mixing ratios. Firstly, the inventory singles out the mobile sources as the primary contributor to NO_x, accounting for 39,000 t year^{-1}, representing 77% of the total emissions (USACH 2014). Also, the number of vehicles has continuously increased over the last decade, reaching a total of 2,124,481 units in 2018 (http://www.ine.cl/) with a maximum increasing rate of 7.8% per year in 2014. Other sectors such as the construction (10%), industrial (10%), residential (4%), and agriculture (0.2%) sectors appear to be less able to explain the increasing NO_x mixing ratios. Therefore, in Santiago, ambient levels of NO_x are highly dependent on motor vehicle emissions.

Similarly, the behavior of CO at the Central Site, another primary pollutant typically emitted by motor engine vehicles, showed a positive trend of (+) 70 [60, 90] ppbv year^{-1} ($p < 0.001$) since 2014, whereas the CO (ppbv) to NO_x (ppbv) ratio during morning rush hour (7:00–9:00) has remained relatively constant over the period 2010–2018 (8.4 with $\sigma = 0.6$) suggesting that the measures implemented in Santiago have contained both CO and NO_x equally.

In Santiago, a significant penetration of diesel motor vehicles has been observed in the national market over the last decade (http://www.ine.cl/). During this period, the number of diesel vehicles doubled since 2009 (198,358), reaching 448,333 units in 2018. Even worse, this growth occurs, disregarding the fact that diesel emits higher NO_x and $PM_{2.5}$ compared with gasoline vehicles.

The incorporation of Talagante station (2010), a peri-urban monitoring station, has been crucial in enabling the characterization of the air that travels into Santiago's basin from the southwest. In this station, the O_3 behavior can be divided into two subsets of data; the first period showed no clear tendency (2010–2013) and the second period (2014–2019) exhibited a statistically significant steady decline of (−) 0.70 [− 0.96, − 0.46] ppbv year^{-1} ($p < 0.001$). Because the Peri-urban Site is located upwind of Central Santiago and could be considered to represent background ozone levels, any O_3 increases in the central area must be independent of background levels. Similarly, the Western monitoring station also showed a declining O_3 mixing ratio trend of (−) 0.31 [− 0.36, − 0.25] ppbv year^{-1} ($p < 0.001$) between 2003 and 2019.

As the predominant near-surface wind in Santiago's basin transports the photochemical plume toward the east of the city (Seguel et al. 2013), the Eastern monitoring station consistently shows the highest levels of O_3 over the last two decades. The O_3 mixing ratio variations by wind speed and wind direction are shown in polar coordinates in Fig. 3. The Eastern Site receives O_3-rich air from Central Santiago mostly during spring, summer, and fall. In winter, wind speed is low (< 3 m/s) and stability high, inhibiting transport (e.g., Mazzeo et al. 2018; Osses et al. 2013). Figure 3 also shows that during the daytime (especially in summer), radiatively driven southwesterly winds lead to the highest ozone levels, as they travel over the city and arrive at the Eastern Site.

At this point, it is worth mentioning that at the time of inception of the monitoring network, the Eastern monitoring station was representative of the eastern part of the city. However, 20 years later, given the expansion of Santiago, a significant part of the north-eastern city is not covered appropriately by the original station network design (Fig. 1).

Trends in O_3 mixing ratio for the Eastern Site showed a decrease of (−) 0.28 ppbv year^{-1} until 2004 (Fig. 2). Between 2005 and 2015, no statistically significant change can be determined, whereas since 2016, O_3 increased at a rate of (+) 1.8 [0.53, 2.6] ppbv year^{-1} at a significance level of 0.01. Unlike the data at Central Santiago, NO and NO_2 levels at the Eastern Site are relatively low, with significant variability. Thus, no trend can be determined for these species during this period (Table 1).

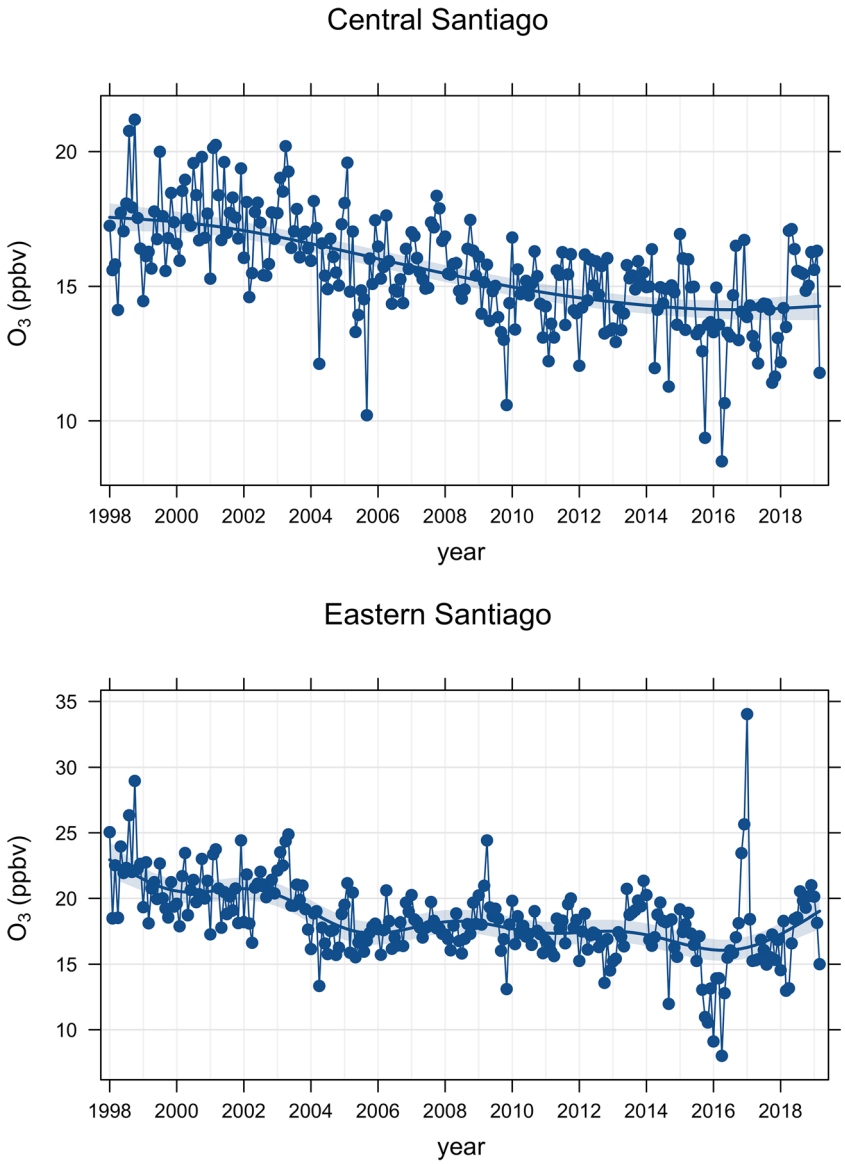

Fig. 2 Trends in O_3 at the Central and Eastern Sites. The plots show the deseasonalized monthly mean mixing ratios of O_3. The shading shows the estimated 95% confidence intervals

Evolution of O_3 primary standard

Figure 4 shows the attainment evaluation of the 8-h O_3 NAAQS. The evaluation was calculated as the 3-year running averages of the 99th percentile (P99) of the MDA8 as described in the "Methodology" section. Remarkable progress has been observed especially in the western and central basin. Significant declines in O_3 mixing ratio have been made possible during the first decade after the implementation of several control measures targeted at reducing PM_{10} (Gallardo et al. 2018). However, cost-effective control strategies on the more reactive VOC emissions have been implemented on a few rare occasions in Santiago to achieve O_3 reductions. One such case was the introduction of vapor capturing devices in most gasoline stations in Santiago in 2008 (Seguel et al. 2012). Furthermore, the ratio of VOC to NO_x has not been explicitly addressed in the attainment plans, and the impact of BVOC emitted from vegetation on O_3 formation remains unknown.

The decade average number days above 61 ppbv per year, expressed as MDA8, has fallen considerably in the last decade compared with the 2000s, from 104 to 43 days at the Eastern Site, from 25 to 4 days at the Central Site, and from 7 to 2 days at the Western Site. However, as indicated in the previous section, the Eastern Site has shown an increase in the second part of the last decade that requires a closer look.

Also, the Receptor Site monitoring station (32° 49' S, 70° 37' W, 819 m altitude) located at the northeast of the Santiago basin in the western foothills of the Andes range (~ 70 km from Santiago) receives the photochemical pollution

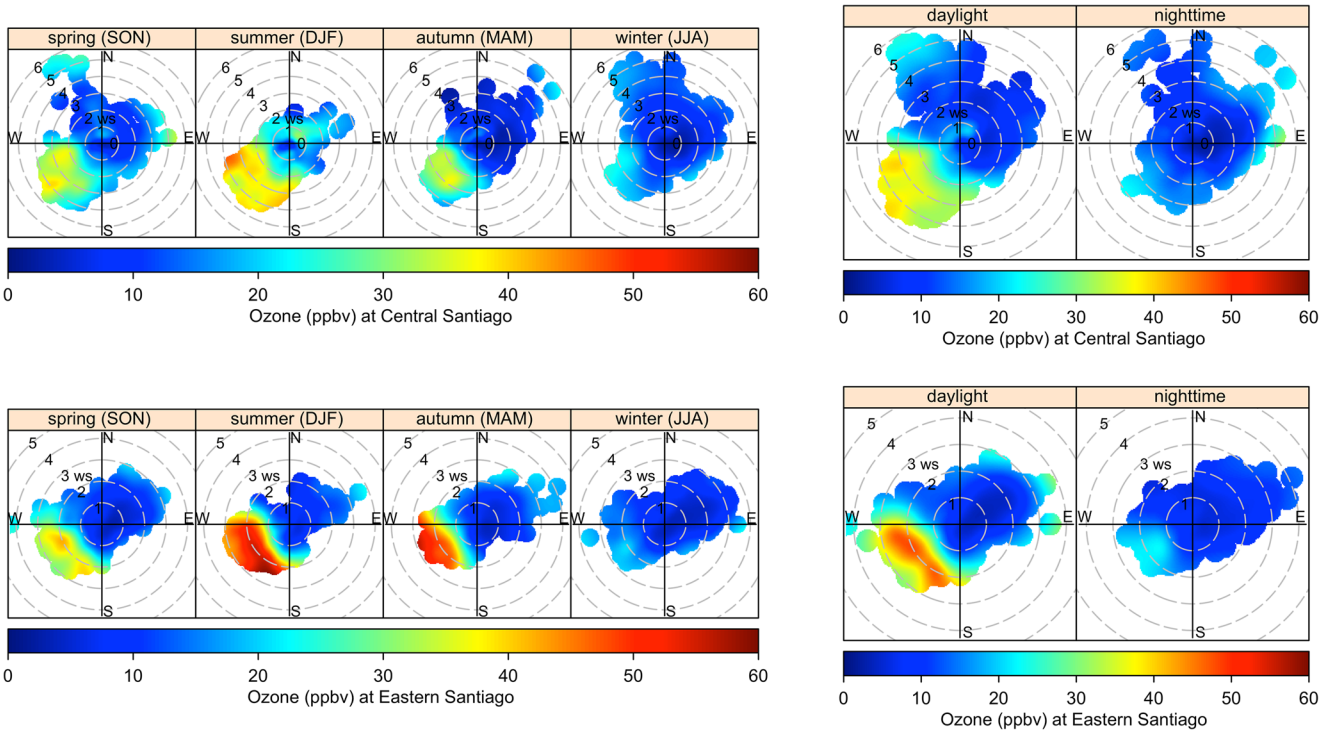

Fig. 3 O_3 mixing ratio variations by wind speed and wind direction in polar coordinates. The plots show variations between 1 January 2014 and 31 March 2019 in the Central and Eastern Sites by season during nighttime or daylight hours as a function of the latitude and longitude in the location (33.5 S, 70.5W)

produced in Santiago especially in the afternoons and evenings when winds tend to be stronger (Seguel et al. 2013). During its first year of O_3 monitoring, it recorded up to 90 days year^{-1} over 61 ppbv of O_3, and therefore it is highly likely that this Receptor Site will be designated as a nonattainment area in the upcoming years (Fig. 5). This demonstrates the importance of addressing not only the pollution in urban areas but also its transport downwind.

VOC to NO_x ratio

Monitoring stations in Santiago show higher levels of O_3 during the weekends compared with weekdays (Seguel et al. 2012). Figure 6 displays the O_3 increase and the drop in NO and NO_2 during weekends in eastern Santiago. The mechanism that produces higher O_3 mixing ratios depends on the VOC to NO_x ratio. At a high enough VOC to NO_x ratio, $^{\bullet}OH$

Table 1 Annual CO to NOx ratio for Wednesdays and Sundays in Central and Eastern Sites

	Central Site						Eastern Site					
	CO Wed	NO_x	CO Sun	NO_x	CO/NO_x Wed	CO/NO_x Sun	CO Wed	NO_x	CO Sun	NO_x	CO/NO_x Wed	CO/NO_x Sun
2010	733	74	751	49	10	15	572	42	481	25	14	20
2011	828	83	824	56	10	15	625	50	461	24	12	19
2012	645	66	680	45	10	15	566	46	494	27	12	18
2013	637	66	711	48	10	15	610	56	486	29	11	17
2014	432	46	523	43	9.3	12	447	43	371	25	10	15
2015	522	60	449	37	8.7	12	480	58	407	29	8.3	14
2016	597	68	510	41	8.8	12	579	53	476	26	11	19
2017	893	78	876	51	11	17	372	45	310	26	8.2	12
2018	742	79	708	52	9.4	13	483	56	401	34	8.6	12
Mean	670	69	670	47	10	14	526	50	432	27	11	16
σ	146	11	147	6	1	2	85	6	63	3	2	3

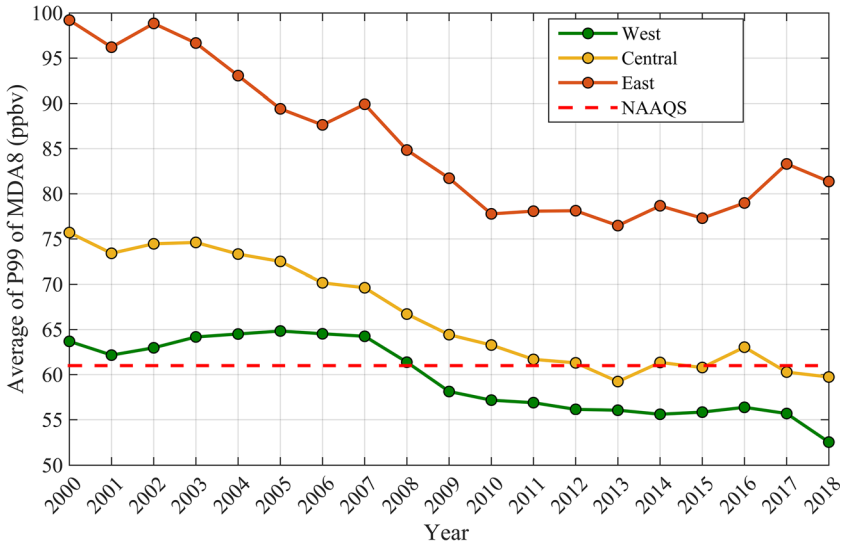

Fig. 4 A 3-year running average evolution of the O_3 standard compliance in the western, central, and eastern Santiago

radicals react mainly with VOCs; conversely, at a low ratio, the NO_x reactions predominate and remove $^{\bullet}OH$ radicals from the system. Thus, under a VOC-limited regime (that is NO_x-saturated), the typical NO reduction that occurs on weekends leads to an increase in O_3 because $^{\bullet}OH$ radicals react preferentially with VOCs and favors a net production of NO_2 (Reactions 2 and 3). Thereby, the subsequent photolysis of NO_2 at wavelengths less than 424 nm produces O_3.

$$RH + {}^{\circ}OH \xrightarrow{O_2} RO_2{}^{\circ} + H_2O \quad (2)$$

$$RO_2{}^{\circ} + 2NO \xrightarrow{O_2} RCHO + 2NO_2 + {}^{\circ}OH \quad (3)$$

In the absence of VOC measurements in Santiago that enable the determination of the VOC to NO_x ratio, CO mixing ratios are useful to provide an insight into the variability of anthropogenic emissions during days of the week. During the 2010s, the CO to NO_x ratio increased respectively by 6, 4, and 5, on Sundays compared with Wednesdays at western, central, and eastern Santiago (Table 1). However, the weekend effect has been more intense in the eastern basin, where the difference between Wednesday and Sunday average O_3 mixing ratio can be higher than 5 ppbv (Fig. 7) due to less inhibition caused by lower NO mixing ratios (Reaction 4) measured in eastern Santiago.

$$NO + O_3 \rightarrow NO_2 + O_2 \quad (4)$$

$$NO_2 + {}^{\circ}OH \rightarrow HONO_2 \quad (5)$$

There are direct health implications for those who perform outdoor recreational activities because O_3 is higher at weekends. Also, the expansion of the city to the northeast implies that more people are potentially susceptible to develop symptoms and effects associated with O_3 exposure. On the other hand, during weekdays, when NO_x is high enough, O_3 is

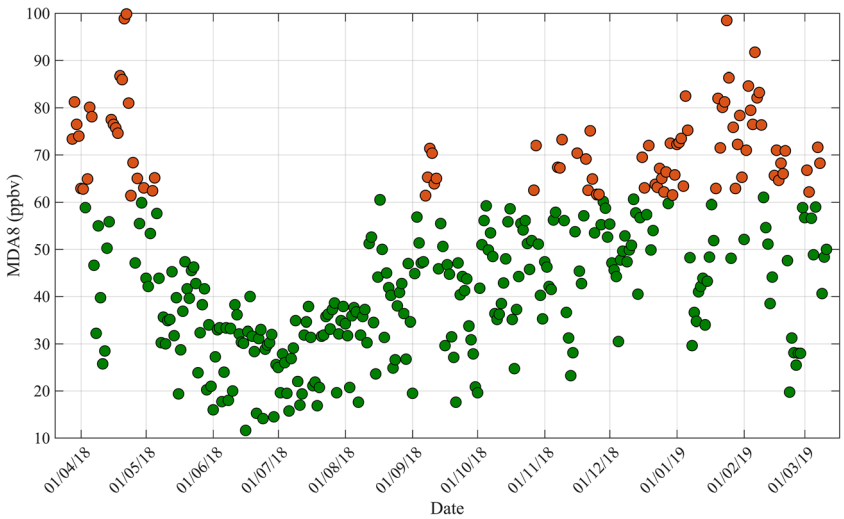

Fig. 5 Maximum daily 8-h average (MDA8) O_3 at the Receptor Site (Los Andes) from April 2018 to March 2019. Red solid dots represent days above 61 ppbv and green solid dots, days of compliance

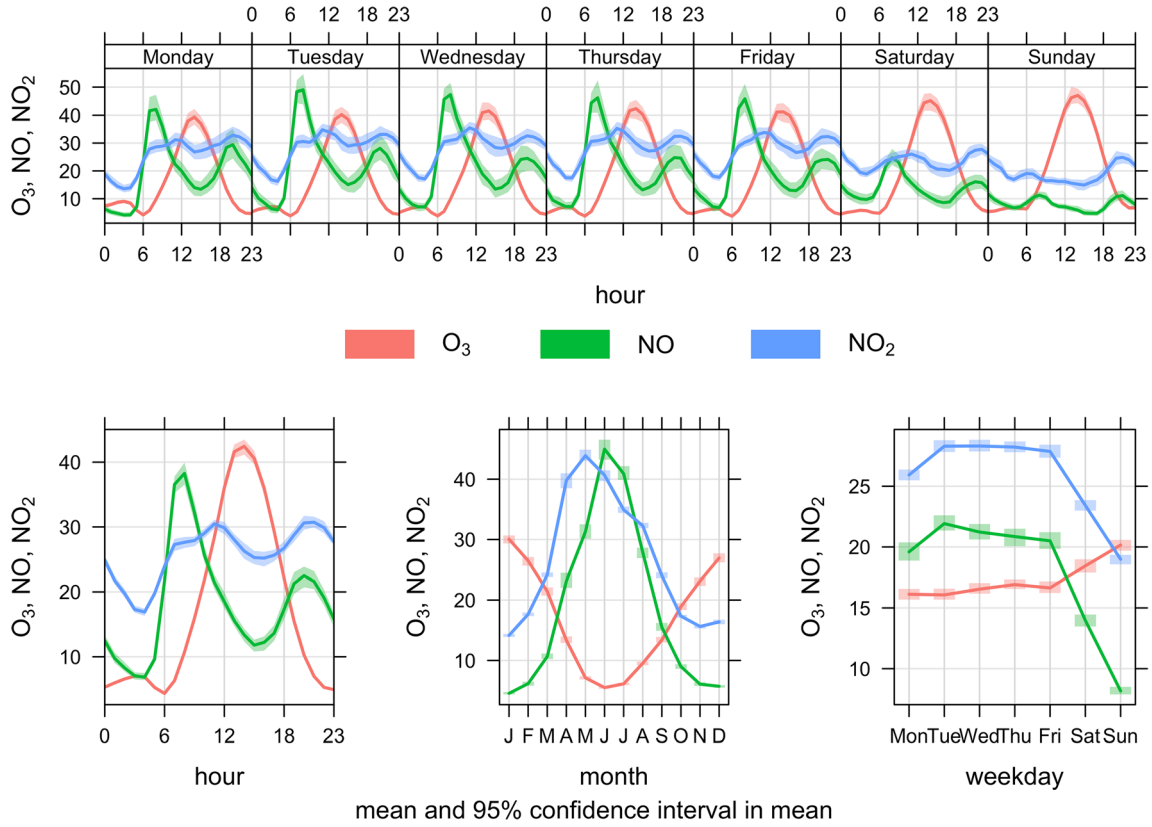

Fig. 6 Variation of O_3, NO, and NO_2 at the Eastern Site between 1 January 2014 and 31 March 2019. The upper panel shows diurnal variation for all days, the bottom left panel shows diurnal variation, the bottom middle panel shows monthly variation, and the bottom right panel shows weekday variation. The shading shows the 95% confidence intervals of the mean

likely titrated by NO, and NO_2 can be removed by reacting with $^{\bullet}OH$ to produce nitric acid (Reaction 5), a toxic air pollutant that is highly water-soluble and therefore harmful to human health and ecosystems (NRC 1983).

As the Santiago Metropolitan Region is VOC-limited, emission control strategies, with greater reductions of NO_x than VOCs, will make it difficult to reduce peak O_3 levels in urban areas. Therefore, future reductions in NO_x must be accompanied by comparable or greater reductions in VOCs. However, reductions in reactive organic gases are challenging in the Santiago basin due to the influence of environmental factors on biogenic VOC emissions.

Heat wave study case (24–28 January 2019)

Central Chile has exhibited an increasing number of heat waves, and projections indicate that heat waves will persist in the future at even higher rates (Ballester et al. 2010; Russo et al. 2014; Bozkurt et al. 2019). There were 10 heat waves during the 2000s during the months of December,

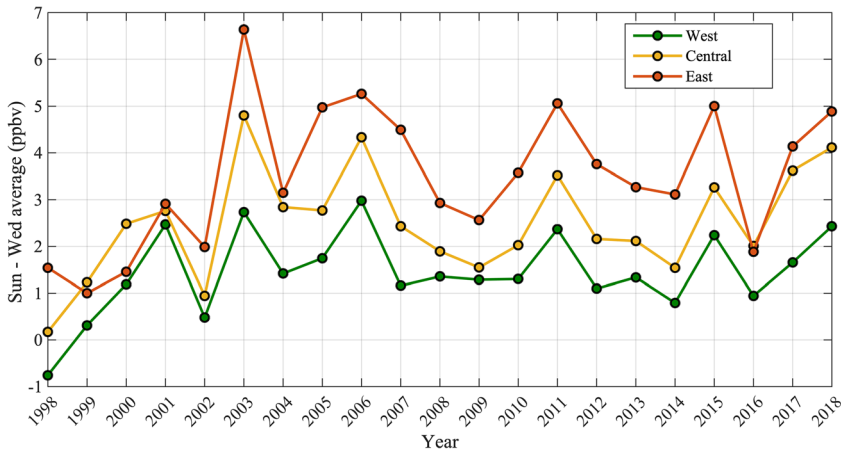

Fig. 7 Difference between Sunday and Wednesday yearly O_3 averages at western, central, and eastern Santiago

Table 2 Heat waves for December, January, and February in central Santiago using the temperature measured by the National Weather Service (available at http://vismet.cr2.cl)

Date	Days	Highest temperature	Date	Days	Highest temperature	Date	Days	Highest temperature
25 Dec 1998	3	33.9	27 Jan 2003	4	36.4	4 Feb 2001	5	33.5
15 Dec 2001	3	34.2	1 Jan 2005	3	35.2	8 Feb 2012	3	34.9
22 Dec 2001	3	33.4	13 Jan 2008	4	34.8	11 Feb 2015	3	35.9
27 Dec 2006	5	34.8	8 Jan 2009	3	33.5	13 Feb 2016	3	34.2
29 Dec 2008	3	34.2	8 Jan 2015	4	35.9	19 Feb 2016	6	34.5
14 Dec 2009	3	34.3	24 Jan 2015	4	33.2	19 Feb 2017	4	34.9
18 Dec 2011	3	32.8	15 Jan 2016	3	35.6	24 Feb 2017	3	32.2
24 Dec 2011	6	33.6	11 Jan 2017	3	35.7	1 Feb 2019	$2^{\dagger}+5$	34.3
27 Dec 2013	4	34.3	17 Jan 2017	5	36.9			
24 Dec 2015	5	35.3	24 Jan 2017	4	37.4			
			29 Jan 2017	$3+1^{\dagger}$	33.9			
			1 Jan 2019	$1^{\dagger}+3$	34.9			
			24 Jan 2019	5	38.3			

† Denotes days from the previous or following month

The table also shows the length of the event and the maximum temperature reached

January, and February (Table 2). In contrast, during the 2010s, that number had grown to 20 episodes. January has been the warmest month and registered the highest temperature since continuous measurements have been available for the Santiago basin, reaching a value of 38.3 °C in 2019.

The most intense heat wave registered in Santiago over the last two decades occurred on 24 January 2019, lasting 5 days. The synoptic-scale conditions associated with this episode shows the presence of a strong high-pressure system that leads to clear skies, especially during the last 3 days of the event. Also, the UV Index was extremely high, reaching values as high as 12, and remaining above 8 between 15:00 and 19:00 h. The UV radiation provides a good indication of how strong the photochemical influence is because the primary source of $^{\bullet}OH$ is the production from the photolysis of O_3, followed by the reaction between excited-state atomic oxygen (O^1D) and water vapor (H_2O) (Reactions 6 and 7). As mentioned in the previous section, the $^{\bullet}OH$ is critical to initiate the VOC oxidations.

$$O_3 + h\nu(\lambda \leq 336nm) \rightarrow O(^1D) + O_2 \quad (6)$$

$$O(^1D) + H_2O \rightarrow 2^{\bullet}OH \quad (7)$$

Figure 8 shows the time series for O_3, NO_2, NO, and temperature for this event. The highest hourly O_3 mixing ratio of 118 ppbv was reached during the hottest day at the Eastern Site (26 January 2019). During Saturday and Sunday, surprisingly, the NO concentration was completely depleted likely due to a total conversion to NO_2 via oxidation of VOCs (Reaction 3). The weekend effect also explains the NO depletion since the NO_x mixing ratio drops significantly in the Eastern Site at weekends (Table 1).

It is also worth noting that during the heat wave episode, the standard can be severely exceeded. Indeed, the MDA8 for the 5 days was higher than 61 ppbv and therefore exceeded the 4 days allowed by the standard (99th percentile) for that particular year.

This case study highlights the more prominent role that will be played by biogenic VOCs and evaporative losses during heat waves and the effect of extreme temperature on the reaction rates leading to increasing O_3 formation and SOA in the Santiago basin. Moreover, the role of biogenic emissions has special relevance in the context of Santiago, where significant differences are found between the southwest and northeast vegetation coverage. The Normalized Different Vegetation Index (NDVI) depicts this remarkable contrast in vegetation abundance (Fig. 1b).

Vegetation-based critical levels: W126 index

W126 critical levels evaluated in the O_3 standard revision by the US EPA (US Federal register 2015) are used in this section as guidelines to interpret the potential impact of O_3 on vegetation. Although in this review, no O_3 secondary standard based on W126 was adopted, the Clean Air Scientific Advisory Committee (CASAC) of the US EPA proposed a range within 7 to 15 ppm-h. Also, to avoid a seasonal W126 index value above a level in the recommended range in any given year of the 3-year period, CASAC advised an upper limit of 13 ppm-h.

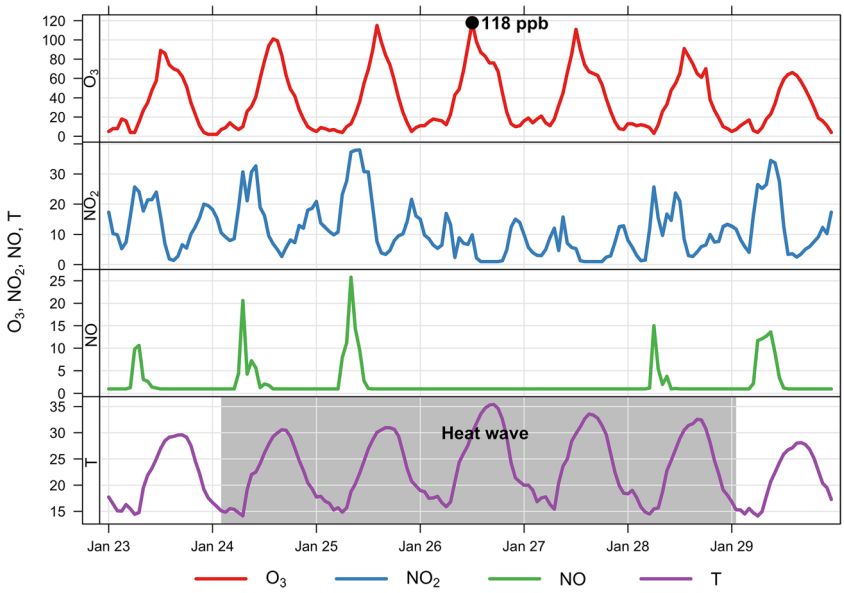

Fig. 8 O_3 response to NO_x changes at the Western Site during a 5-day heat wave in Central Chile. The shaded area represents the heat wave period. The hourly maximum mixing ratio of O_3 is highlighted by a solid dot

The trend of the W126 index for Peri-urban, Western, Central, and Eastern Sites is shown in Fig. 9. In the peri-urban monitoring station, the 3-year average of W126 is 3 ppm-h or below. Also, western and central Santiago showed values below the CASAC advice of 13 ppm-h. By contrast, in the eastern part of Santiago, the 3-year average of W126 has exceeded the guideline since 2000, with the worst performance observed during the 2000s. A deeper look at the Eastern Site data shows a significant fluctuation in recent years. For instance, the highest 3-month sum for 2015, 2016, 2017, and 2018 is 18, 16, 24, and 10 ppm-h, respectively. This variability may be associated with the effect of warmer summers (e.g., 2017) and requires further research regarding the role of biogenic VOCs and pyrogenic species emitted by the wildfires that occurred over these seasons (de la Barrera et al. 2018). However, in light of the results, one may claim that cropland and forest trees located downwind of Santiago have been and still are potentially subject to the injurious effects of O_3 and other photochemical oxidants. This risk might be a matter of concern for the Chilean productivity as the export of fruit is a significant part of the national economy (http://www.bcentral.cl/comercio-exterior).

Additionally, the comparison between O_3 NAAQS and the W126 index in the 2010s shows that NAAQS compliance can also have the potential to protect vegetation. For example, the Western Site met the NAAQS as well as the W126 threshold of 13 ppm-h. However, unlike other international legislation, the Chilean O_3 standard does not address the effects on ecosystems, and the focus is exclusively targeted on public health.

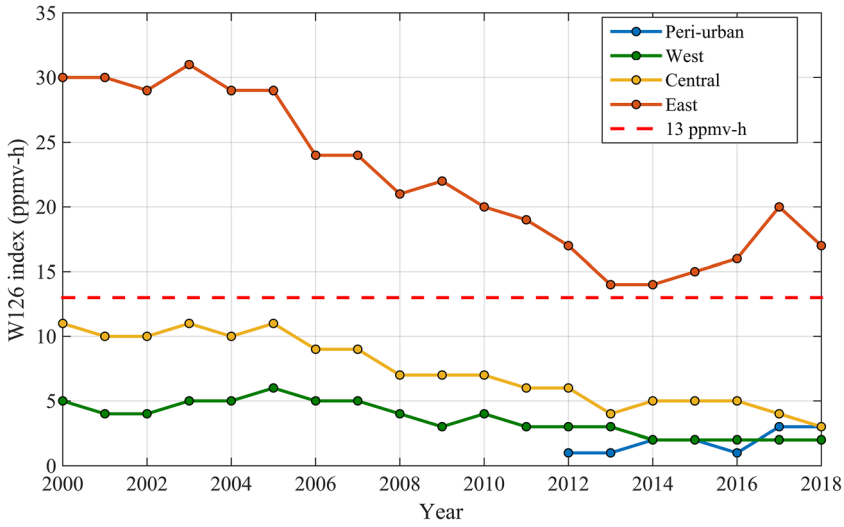

Fig. 9 A 3-year average of W126 computed using hourly O_3 mixing ratio in Santiago

Conclusions

Central Santiago will continue to be close to the O_3 standard, while eastern Santiago will probably exceed it as long as the current increasing trend in the mobile source emissions, consisting primarily of gasoline motor engines and secondly of diesel motor engines, continues to grow. Therefore, to reduce population exposure to O_3 and other hazardous photochemical products, it is essential to strongly reduce the emissions of VOCs and NO_x by introducing cleaner transportation on a large scale.

The emergence of heat waves and their effect on increasing biogenic emissions and anthropogenic evaporative losses will continue to be a determining factor for compliance of the O_3 standard. Currently the 4 permitted days above 61 ppbv per year are consistently exceeded during a typical heat wave episode. This shows the need to distinguish between episodes that are attributable to direct anthropogenic emissions from those that are associated with a changing climate and weather that need to be addressed using a different approach.

Due to the various different natural and man-made processes occurring in Santiago such as the predominant wind, heat waves, weekend effect, and the increasing development of the city toward the north-eastern part of the basin, it is necessary to implement measures that protect sensitive populations against the risk of exposure to oxidants as well as to communicate the risk associated.

The design of the current air quality-monitoring network needs an improved spatial coverage, taking into account the transport of photochemical pollutants as well as the current urban development of the city. Also, cost-effective measures that could achieve an O_3 reduction in Santiago demand a fundamental description of the organic atmospheric composition.

The secondary index (W126) for O_3 shows the urgency of transitioning from a local urban pollution approach to a regional one based on the notorious air pollution transport observed between the central valleys of Chile that not only influences the health of sensitive groups but also the agricultural crop yields in one of the most productive areas of the country.

Acknowledgments We thank Camilo Menares for assistance in plotting topography in Fig. 1a. We also thank Pamela Smith for plotting the NDVI in Fig. 1b.

Funding information This work has been funded by ANID/FONDAP/15110009 and PAPILA (Prediction of Air Pollution in Latin America and the Caribbean) project (ID: 777544, H2020-EU.1.3.3.).

References

Atkinson R, Arey J (1998) Atmospheric chemistry of biogenic organic compounds. Acc Chem Res 31:574–583. https://doi.org/10.1021/ar970143z

Atkinson R, Arey J (2003) Gas-phase tropospheric chemistry of biogenic volatile organic compounds: a review. Atmos Environ 37:197–219. https://doi.org/10.1016/S1352-2310(03)00391-1

Ballester J, Rodó X, Giorgi F (2010) Future changes in Central Europe heat waves expected to mostly follow summer mean warming. Clim Dyn 35:1191–1205. https://doi.org/10.1007/s00382-009-0641-5

Barraza F, Lambert F, Jorquera H, Villalobos AM, Gallardo L (2017) Temporal evolution of main ambient PM2. 5 sources in Santiago, Chile, from 1998 to 2012. Atmos Chem Phys 17:10093–10107. https://doi.org/10.5194/acp-17-10093-2017

Bell ML, McDermott A, Zeger SL, Samet JM, Dominici F (2004) OZone and short-term mortality in 95 us urban communities, 1987-2000. JAMA 292:2372–2378. https://doi.org/10.1001/jama.292.19.2372

Boisier JP, Rondanelli R, Garreaud RD, Muñoz F (2016) Anthropogenic and natural contributions to the Southeast Pacific precipitation decline and recent megadrought in Central Chile. Geophys Res Lett 43:413–421. https://doi.org/10.1002/2015gl067265

Boisier JP, Alvarez-Garretón C, Cordero RR, Damiani A, Gallardo L, Garreaud RD, Lambert F, Ramallo C, Rojas M, Rondanelli R (2018) Anthropogenic drying in Central-Southern Chile evidenced by long-term observations and climate model simulations. Elem Sci Anth 6(1):74. https://doi.org/10.1525/elementa.328

Bozkurt D, Rojas M, Boisier JP, Rondanelli R, Garreaud R, Gallardo L (2019) Dynamical downscaling over the complex terrain of southwest South America: present climate conditions and added value analysis. Clim Dyn 53:6745–6767. https://doi.org/10.1007/s00382-019-04959-y

Carslaw DC (2013) The Openair manual: open-source tools for analyzing air pollution data. Manual for version 0.9. King's College London. London, UK. [WWW document] URL https://goo.gl/iigCI9 (accessed 5 January 2018)

de la Barrera F, Barraza F, Favier P, Ruiz V, Quense J (2018) Megafires in Chile 2017: Monitoring multiscale environmental impacts of burned ecosystems. Sci Total Environ 637-638:1526–1536. https://doi.org/10.1016/j.scitotenv.2018.05.119

DMC (2018) Reporte meteorológico available at: https://climatologia.meteochile.gob.cl/application/publicaciones/reporteClimatologico/2018. Accessed 1 Nov 2019

Elshorbany YF et al (2009) Summertime photochemical ozone formation in Santiago. Chile Atmos Environ 43:6398–6407. https://doi.org/10.1016/j.atmosenv.2009.08.047

Elshorbany YF et al (2010) Seasonal dependence of the oxidation capacity of the city of Santiago de Chile. Atmos Environ 44:5383–5394. https://doi.org/10.1016/j.atmosenv.2009.08.036

Entwistle MR, Gharibi H, Tavallali P, Cisneros R, Schweizer D, Brown P, Ha S (2019) Ozone pollution and asthma emergency department visits in Fresno, CA, USA, during the warm season (June–September) of the years 2005 to 2015: a time-stratified case-crossover analysis. Air Qual Atmos Health 12:661–672. https://doi.org/10.1007/s11869-019-00685-w

Falvey M, Garreaud RD (2009) Regional cooling in a warming world: recent temperature trends in the southeast Pacific and along the west coast of subtropical South America (1979–2006). J Geophys Res: Atmospheres 114 doi:https://doi.org/10.1029/2008jd010519

Gallardo L, Olivares G, Langner J, Aarhus B (2002) Coastal lows and sulfur air pollution in Central Chile. Atmos Environ 36:3829–3841. https://doi.org/10.1016/S1352-2310(02)00285-6

Gallardo L, Barraza F, Ceballos A, Galleguillos M, Huneeus N, Lambert F, Ibarra C, Munizaga M, O'Ryan R, Osses M, Tolvett S, Urquiza A, Véliz KD (2018) Evolution of air quality in Santiago: the role of mobility and lessons from the science-policy interface. Elem Sci Anth 6(1):38. https://doi.org/10.1525/elementa.293

Garreaud R, Rutllant J, Fuenzalida H (2002) Coastal lows along the subtropical west coast of South America: mean structure and evolution. Mon Weather Rev 130:75–88. https://doi.org/10.1175/1520-0493(2002)130<0075:clatsw>2.0.co;2

Garreaud RD, Vuille M, Compagnucci R, Marengo J (2009) Present-day South American climate Palaeogeography. Palaeoclimatol Palaeoecol 281:180–195. https://doi.org/10.1016/j.palaeo.2007.10.032

GBD (2016) Global, regional, and national comparative risk assessment of 84 behavioural, environmental and occupational, and metabolic risks or clusters of risks, 1990–2016: a systematic analysis for the Global Burden of Disease Study 2016. Lancet 2017 390:1345–1422

Goldstein AH, Galbally IE (2007) Known and unexplored organic constituents in the Earth's. Atmos Environ Sci Technol 41:1514–1521. https://doi.org/10.1021/es072476p

Jimenez JL, Canagaratna MR, Donahue NM, Prevot AS, Zhang Q, Kroll JH, DeCarlo P, Allan JD, Coe H, Ng NL, Aiken AC, Docherty KS, Ulbrich IM, Grieshop AP, Robinson AL, Duplissy J, Smith JD, Wilson KR, Lanz VA, Hueglin C, Sun YL, Tian J, Laaksonen A, Raatikainen T, Rautiainen J, Vaattovaara P, Ehn M, Kulmala M, Tomlinson JM, Collins DR, Cubison MJ, Dunlea EJ, Huffman JA, Onasch TB, Alfarra MR, Williams PI, Bower K, Kondo Y, Schneider J, Drewnick F, Borrmann S, Weimer S, Demerjian K, Salcedo D, Cottrell L, Griffin R, Takami A, Miyoshi T, Hatakeyama S, Shimono A, Sun JY, Zhang YM, Dzepina K, Kimmel JR, Sueper D, Jayne JT, Herndon SC, Trimborn AM, Williams LR, Wood EC, Middlebrook AM, Kolb CE, Baltensperger U, Worsnop DR (2009) Evolution of organic aerosols in the atmosphere. Science 326:1525–1529. https://doi.org/10.1126/science.1180353

Lee JD et al (2006) Ozone photochemistry and elevated isoprene during the UK heatwave of august 2003. Atmos Environ 40:7598–7613. https://doi.org/10.1016/j.atmosenv.2006.06.057

Lefohn AS, Runeckles VC (1987) Establishing standards to protect vegetation—ozone exposure/dose considerations. Atmos Environ (1967) 21:561–568. https://doi.org/10.1016/0004-6981(87)90038-2

Lippmann M (1991) Health effects of tropospheric ozone. Environ Sci Technol 25:1954–1962. https://doi.org/10.1021/es00024a001

Liu JC, Peng RD (2018) Health effect of mixtures of ozone, nitrogen dioxide, and fine particulates in 85 US counties. Air Qual Atmos Health. https://doi.org/10.1007/s11869-017-0544-2

Mazzeo A et al (2018) Impact of residential combustion and transport emissions on air pollution in Santiago during winter. Atmos Environ 190:195–208. https://doi.org/10.1016/j.atmosenv.2018.06.043

McConnell R, Berhane K, Gilliland F, London SJ, Islam T, Gauderman WJ, Avol E, Margolis HG, Peters JM (2002) Asthma in exercising children exposed to ozone: a cohort study. Lancet 359:386–391

Mena-Carrasco M et al (2014) Regional climate feedbacks in Central Chile and their effect on air quality episodes and meteorology. Urban Clim 10:771–781. https://doi.org/10.1016/j.uclim.2014.06.006

Mills G, Pleijel H, Malley CS, Sinha B, Cooper OR, Schultz MG, Neufeld HS, Simpson D, Sharps K, Feng Z, Gerosa G, Harmens H, Kobayashi K, Saxena P, Paoletti E, Sinha V, Xu X (2018) Tropospheric ozone assessment report: present-day tropospheric ozone distribution and trends relevant to vegetation. Elem Sci Anth 6(1):47. https://doi.org/10.1525/elementa.302

NRC (1983) Acid deposition: atmospheric processes in Eastern North America. National Academy Press, Washington

Osses A, Gallardo L, Faundez T (2013) Analysis and evolution of air quality monitoring networks using combined statistical information indexes. Tellus Ser B Chem Phys Meteorol 65:19822. https://doi.org/10.3402/tellusb.v65i0.19822

Paasonen P et al (2013) Warming-induced increase in aerosol number concentration likely to moderate climate change. Nat Geosci 6:438. https://doi.org/10.1038/ngeo1800 https://www.nature.com/articles/ngeo1800#supplementary-information

Piticar A (2018) Changes in heat waves in Chile. Glob Planet Chang 169:234–246. https://doi.org/10.1016/j.gloplacha.2018.08.007

Préndez M, Carvajal V, Corada K, Morales J, Alarcón F, Peralta H (2013) Biogenic volatile organic compounds from the urban forest of the Metropolitan Region. Chile Environ Poll 183:143–150. https://doi.org/10.1016/j.envpol.2013.04.003

Rappenglück B, Oyola P, Olaeta I, Fabian P (2000) The evolution of photochemical smog in the Metropolitan Area of Santiago de Chile. J Appl Meteorol 39:275–290. https://doi.org/10.1175/1520-0450(2000)039<0275:TEOPSI>2.0.CO;2

Rappenglück B et al (2005) An urban photochemistry study in Santiago de Chile. Atmos Environ 39:2913–2931. https://doi.org/10.1016/j.atmosenv.2004.12.049

Rubio M, Oyola P, Gramsch E, Lissi E, Pizarro J, Villena G (2004) Ozone and peroxyacetylnitrate in downtown Santiago. Chile Atmos Environ 38:4931–4939. https://doi.org/10.1016/j.atmosenv.2004.05.051

Russo S et al (2014) Magnitude of extreme heat waves in present climate and their projection in a warming world. J Geophys Res-Atmos 119:12,500–512,512. https://doi.org/10.1002/2014jd022098

Saide PE, Carmichael GR, Spak SN, Gallardo L, Osses AE, Mena-Carrasco MA, Pagowski M (2011) Forecasting urban PM10 and PM2.5 pollution episodes in very stable nocturnal conditions and complex terrain using WRF–Chem CO tracer model. Atmos Environ 45:2769–2780. https://doi.org/10.1016/j.atmosenv.2011.02.001

Schultz MG et al (2017) Tropospheric ozone assessment report: database and metrics data of global surface ozone observations. Elem Sci Anth 5:58. https://doi.org/10.1525/elementa.244

Scott CE, Arnold SR, Monks SA, Asmi A, Paasonen P, Spracklen DV (2018) Substantial large-scale feedbacks between natural aerosols and climate. Nat Geosci 11:44–48. https://doi.org/10.1038/s41561-017-0020-5

Seguel RJ, Morales R, Leiva M (2009) Estimations of primary and secondary organic carbon formation in PM2.5 aerosols of Santiago City, Chile. Atmos Environ 43:2125–2131. https://doi.org/10.1016/j.atmosenv.2009.01.029

Seguel RJ, Morales SR, Leiva GM (2012) Ozone weekend effect in Santiago. Chile Environ Pollut 162:72–79. https://doi.org/10.1016/j.envpol.2011.10.019

Seguel RJ, Mancilla C, Rondanelli R, Leiva M, Morales R (2013) Ozone distribution in the lower troposphere over complex terrain in Central Chile. J Geophys Res-Atmos 118:2966–2980. https://doi.org/10.1002/jgrd.50293

Seguel RJ, Mancilla C, MAL G (2018) Stratospheric ozone intrusions during the passage of cold fronts over Central Chile. Air Qual Atmos Health 11:535–548. 1–14. https://doi.org/10.1007/s11869-018-0558-4

Shrivastava M et al (2017) Recent advances in understanding secondary organic aerosol: implications for global climate forcing. Rev Geophys 55:509–559. https://doi.org/10.1002/2016rg000540

Toro R, Donoso C, Seguel R, Morales RES, Leiva MG (2014) Photochemical ozone pollution in the Valparaiso Region, Chile. Air Qual Atmos Health 7:1–11. https://doi.org/10.1007/s11869-013-0218-7

Toro AR, Seguel R, Morales SRE, Leiva GM (2015) Ozone, nitrogen oxides, and volatile organic compounds in a central zone of Chile. Air Qual Atmos Health 8:545–557 1-13. https://doi.org/10.1007/s11869-014-0306-3

Tsigaridis K, Kanakidou M (2018) The present and future of secondary organic aerosol direct forcing on climate. Curr Clim Change Rep 4:84–98. https://doi.org/10.1007/s40641-018-0092-3

US Federal Register. (2015) National Ambient Air Quality Standards for Ozone, 40 CFR Part 50, 51, 52, 53, and 58, 65292–65468

USACH (2014) Actualización y sistematización del inventario de emisiones de contaminantes atmosféricos en la Región Metropolitana. Ministerio de medio Ambiente. Available at: http://

metadatos.mma.gob.cl/servicios/metadata/recursos/downloadRecurso/324084/USACH_Inf_Inventarios_FINAL.pdf. Accessed 1 Nov 2019

Van Dingenen R, Dentener FJ, Raes F, Krol MC, Emberson L, Cofala J (2009) The global impact of ozone on agricultural crop yields under current and future air quality legislation. Atmos Environ 43:604–618. https://doi.org/10.1016/j.atmosenv.2008.10.033